Available online at www.sciencedirect.com
ScienceDirect
Chaos, Solitons and Fractals 39 (2009) 1092–1099
CHAOS
SOLITONS & FRACTALS
www.elsevier.com/locate/chaos

Effect of nonlinear dissipation on the basin boundaries of a driven two-well Rayleigh–Duffing oscillator

M. Siewe Siewe [a], Hongjun Cao [b,c], Miguel A.F. Sanjuán [c,*]

[a] Laboratoire de Mécanique, Département de Physique, Faculté des sciences, Université de Yaoundé I, B.P. 812 Yaoundé, Cameroon
[b] Department of Mathematics, School of Science, Beijing Jiaotong University, Beijing 100044, PR China
[c] Nonlinear Dynamics and Chaos Group, Departamento de Física, Universidad Rey Juan Carlos, Tulipán s/n, 28933 Móstoles, Madrid, Spain

Accepted 30 April 2007

Abstract

The Rayleigh oscillator is one canonical example of self-excited systems. However, simple generalizations of such systems, such as the Rayleigh–Duffing oscillator, have not received much attention. The presence of a cubic term makes the Rayleigh–Duffing oscillator a more complex and interesting case to analyze. In this work, we use analytical techniques such as the Melnikov theory, to obtain the threshold condition for the occurrence of Smale-horseshoe type chaos in the Rayleigh–Duffing oscillator. Moreover, we examine carefully the phase space of initial conditions in order to analyze the effect of the nonlinear damping, and in particular how the basin boundaries become fractalized.

1. Introduction

The forced and damped Duffing oscillator has served as a prototype model for various physical and engineering problems such as Josephson junctions, optical bistability, plasma oscillations, buckled beam, and electrical circuit [1–12]. Since Ueda's work in 1979 [13], it is known that chaotic responses are commonplace in Duffing oscillators subjected to a harmonic perturbation.

Usually, the phenomenological model of the dissipative force is assumed to be linear with respect to the velocity. In this context it is appropriate to recall the words of Pippard [15]: *There is something of a tendency among physicists to try to reduce everything to linearity…, reality may not always conform to what might wish, rather more so with the damping forces than with the restoring force in small-amplitude vibrations.*

Several phenomenological models of nonlinear damping are given in the literature [8,14]. In this paper, the dissipative force is assumed to be nonlinear, and its main feature is to be a self-excited system like the Van der Pol oscillator. We examine the effect of the damping coefficient on the Duffing oscillator by introducing a cubic power of the velocity in the dissipative function, the so-called Rayleigh dissipation. The resultant equation of motion is given by

$$\ddot{x} - \mu(1 - \dot{x}^2)\dot{x} - x + x^3 = F\cos\omega t, \tag{1}$$

* Corresponding author.
E-mail address: miguel.sanjuan@urjc.es (M.A.F. Sanjuán).

0960-0779/$ - see front matter © 2007 Elsevier Ltd. All rights reserved.
doi:10.1016/j.chaos.2007.05.007

where μ is a real parameter, and F and ω are respectively the amplitude and the frequency of the external perturbation. Moreover, the system is invariant under the transformation of $x \to -x$, and $t \to t + \pi/\omega$. The Rayleigh oscillator [16] is like the Van der Pol oscillator save one key difference: as the voltage increases, the Van der Pol oscillator increases in frequency while the Rayleigh oscillator increases in amplitude. This system is of real physical interest, since it might be useful to model many physical and engineering systems, and in the context of chemical and biological oscillators. Much work has been done on the mechanisms by which the strange attractors arise and are modified as a parameter of the system is varied. These mechanisms include period-doubling cascades, intermittency, crisis, etc. As an example of applications of this model, Yamapi [17] has studied the stability of the synchronization process in a ring of four mutually coupled self-sustained electrical systems described by the coupled Rayleigh–Duffing equations. In their work, Wang et al. [18] have considered the dynamics of a micro-electromechanical system (MEMS) device, and it has been shown that with two separate actuators generating the force, a double-well potential can be formed as those appearing in the Duffing oscillator.

Our goal in this paper is to make a contribution in the study of the transition to chaos in the Rayleigh–Duffing oscillator by using the Melnikov theory, and then see how the fractal basin boundaries arise and are modified as the damping coefficient is varied. The last part of this work consists of a numerical investigation of the strange attractor at parameter values which are close to the analytically predicted bifurcation curves. In particular, the case of the two-well potential is considered.

This paper is organized as follows: In Section 2 we deal with the description, analysis of the model, and some comparison with the Rayleigh oscillator. In Section 3, the conditions for the existence of chaos are thoroughly analyzed. A convenient demonstration of the accuracy of the method is obtained from the fractal basin boundaries, and this is discussed in Section 4. Finally we summarize our results in Section 5.

2. Description and analysis of the model

We are considering here the Rayleigh–Duffing oscillator, which is given by

$$\ddot{x} - \mu(1 - \dot{x}^2)\dot{x} - x + x^3 = F\cos\omega t. \tag{2}$$

This equation possesses a nonlinear damping term and a nonlinear restoring force. The nonlinear damping term corresponds to the Rayleigh oscillator including a cubic term of the velocity, while the nonlinear restoring force corresponds to the Duffing oscillator, hence its name. The unperturbed forced Rayleigh oscillator, that is, in the absence of the cubic nonlinearities in the restoring force of Eq. (1), possesses only one hyperbolic equilibrium point $(0,0)$.

We next derive the fixed points and the phase portrait corresponding to the unperturbed system. If we let $\mu = F = 0$, the unperturbed system can be written as

$$\dot{x} = y, \quad \dot{y} = x - x^3, \tag{3}$$

which corresponds to an integrable Hamiltonian system with the potential function given by

$$V(x) = -\frac{1}{2}x^2 + \frac{1}{4}x^4, \tag{4}$$

whose associated Hamiltonian function is

$$H(x,y) = \frac{1}{2}y^2 - \frac{1}{2}x^2 + \frac{1}{4}x^4. \tag{5}$$

By analyzing the unperturbed system, we can observe that there are three different equilibria: one hyperbolic equilibrium point $(0,0)$, and two elliptic points. The saddle is connected by two symmetric homoclinic orbits as shown in Fig. 1b.

We next compare the unforced Rayleigh oscillator $\ddot{x} - (1 - \dot{x}^2)\dot{x} - x = 0$ and the unforced Rayleigh–Duffing oscillator $\ddot{x} - 0.02(1 - \dot{x}^2)\dot{x} - x + x^3 = 0$.

We rewrite the unforced Rayleigh oscillator $\ddot{x} - (1 - \dot{x}^2)\dot{x} - x = 0$ as the following formula

$$\dot{x} = y, \quad \dot{y} = x - (1 - y^2)y, \tag{6}$$

which possesses only one hyperbolic saddle point $(0,0)$, while corresponding to the unforced Rayleigh–Duffing oscillator $\ddot{x} - 0.02(1 - \dot{x}^2)\dot{x} - x + x^3 = 0$ and its equivalent form

$$\dot{x} = y, \quad \dot{y} = x - x^3 + (1 - y^2)y, \tag{7}$$

possess three different equilibria: one hyperbolic equilibrium point $(0,0)$, and two elliptic points. Fig. 2 represents the corresponding phase portraits between the unforced Rayleigh oscillator and the unforced Rayleigh–Duffing oscillator, respectively.

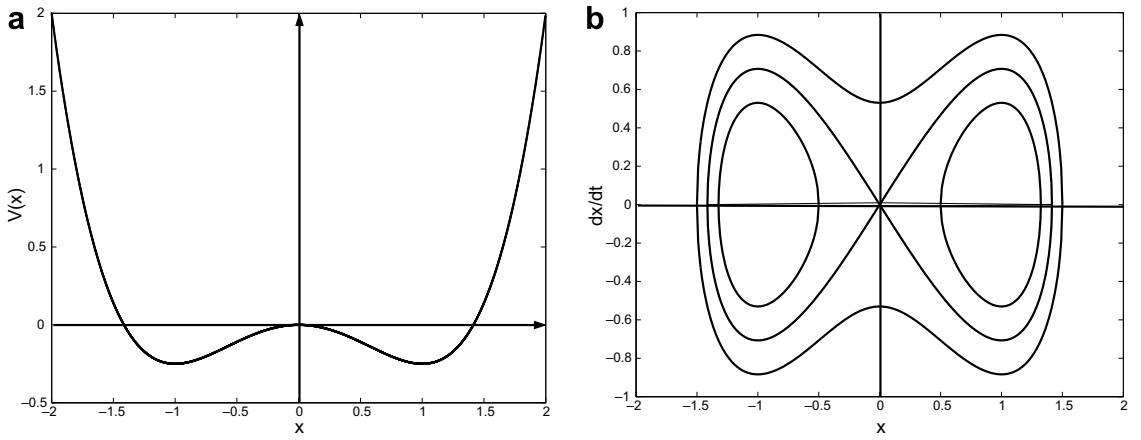

Fig. 1. (a) The two-well potential function of the unperturbed system (3); (b) the corresponding phase space portrait of the unperturbed system (3).

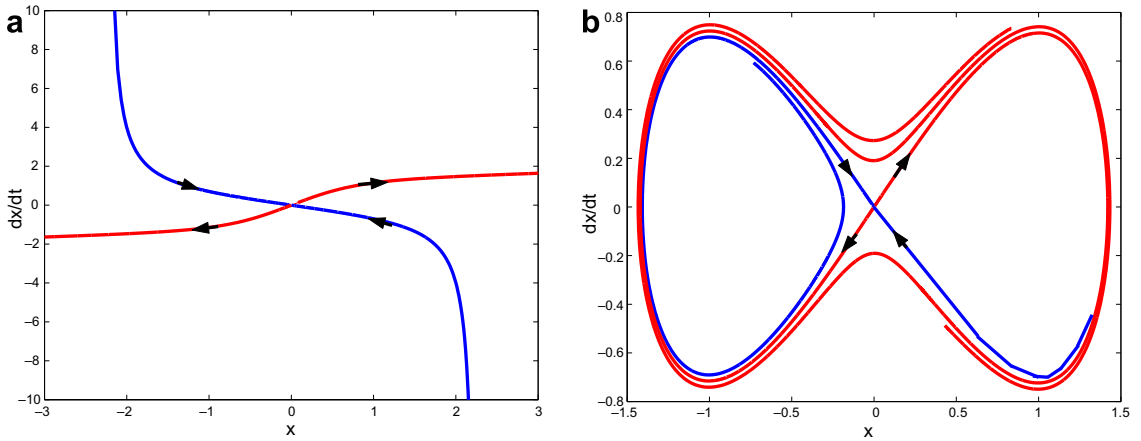

Fig. 2. (a) Phase portrait of the unforced Rayleigh oscillator $\ddot{x} - (1 - \dot{x}^2)\dot{x} - x = 0$; (b) phase portrait of the unforced Rayleigh–Duffing oscillator $\ddot{x} - 0.02(1 - \dot{x}^2)\dot{x} - x + x^3 = 0$.

3. Taming chaotic behavior in the Rayleigh–Duffing oscillator

The generalized Melnikov method developed by Wiggins [19] consists of studying a system, that when unperturbed is an integrable Hamiltonian system having a normally hyperbolic invariant set, whose stable and unstable manifold intersect non-transversely. The structure of the unperturbed system corresponds to two uncoupled one-degree of freedom Hamiltonian systems. In this section, we discuss the chaotic behavior of the system

$$\ddot{x} - \mu(1 - \dot{x}^2)\dot{x} - x + x^3 = F\cos\omega t, \tag{8}$$

in which μ and F are assumed to be small parameters. Hence, our dynamical system may be written as

$$\begin{cases} \dot{x} = y, \\ \dot{y} = x - x^3 + (\mu(1 - y^2)y + F\cos z), \\ \dot{z} = \omega. \end{cases} \tag{9}$$

When the perturbations are added, the homoclinic orbit might be broken transversely. And then, by the Smale–Birkhoff Theorem [19], horseshoe type chaotic dynamics may appear. It is well known, that the predictions for the appearance of chaos are limited, and only valid for orbits starting at points sufficiently close to the separatrix. On the other hand it constitutes a first order perturbation method. Although the chaos does not manifest itself in the form of permanent

chaos, and some sorts of transient chaos may show up. However, it manifest itself in terms of the fractal basin boundaries, as it was shown by [20].

Considering Eq. (5), we see that the unperturbed Rayleigh–Duffing oscillator has a hyperbolic fixed point at the origin $(x, \dot{x}) = (0, 0)$ in the phase space connected to itself by symmetric homoclinic orbits, which is the basic requirement for the application of the Melnikov method. Then the equations for the homoclinic orbits are defined as

$$(x_h, y_h) = \left(\pm\sqrt{2}\,\mathrm{sech}\, t, \mp\sqrt{2}\,\mathrm{sech}\, t \tanh t\right). \tag{10}$$

We apply the Melnikov method to our system in order to find the necessary criteria for the existence of homoclinic bifurcations and chaos. The Melnikov integral is defined as

$$M(t_0) = \mu \int y_h^2 \,\mathrm{d}t - \mu \int y_h^4 \,\mathrm{d}t + F \int y_h \cos\omega(t + t_0)\,\mathrm{d}t, \tag{11}$$

where t_0 is the cross-section time of the Poincaré map and t_0 can be interpreted as the initial time of the forcing term. After substituting the equations of the homoclinic orbits x_h and y_h given in Eq. (10) into Eq. (11) and evaluating the corresponding integral, we obtain the Melnikov function given by

$$M(t_0) = \mu I_0 - \mu I_1 + F I_2 \sin\omega t_0, \tag{12}$$

where

$$\begin{aligned} I_0 &= 2\int_{-\infty}^{+\infty} \mathrm{sech}^2(t)\tanh^2 t\,\mathrm{d}t, \\ I_1 &= 4\int_{-\infty}^{+\infty} \mathrm{sech}^4(t)\tanh^4 t\,\mathrm{d}t, \\ I_2 &= -\sqrt{2}\int_{-\infty}^{+\infty} \mathrm{sech}(t)\tanh t \sin\omega t\,\mathrm{d}t. \end{aligned} \tag{13}$$

After evaluation of these elementary integrals, the Melnikov function is computed. It is known, that the intersections of the homoclinic orbits are the necessary conditions for the existence of chaos. The Melnikov function theory measures the distance between the perturbed stable and unstable manifolds in the Poincaré section. If $M(t_0)$ has a simple zero, then a homoclinic bifurcation occurs, signifying the possibility of chaotic behavior. This means that only necessary conditions for the appearance of strange attractors are obtained from the Poincaré–Melnikov–Arnold analysis, and therefore one has always the chance of finding the sufficient conditions for the elimination of even transient chaos. Then the necessary condition for which the invariant manifolds intersect themselves is given by

$$\mu = \frac{3\sqrt{2}F\pi\omega}{8}\mathrm{sech}\frac{\pi\omega}{2}. \tag{14}$$

This implies that if the perturbation is sufficiently small, the reduced Eq. (9) has transverse homoclinic orbits resulting in possible chaotic dynamics. We study the chaotic threshold as a function of only the frequency parameter ω. A typical plot of μ against ω is shown in Fig. 3, in which the critical homoclinic bifurcation curves are plotted versus the fre-

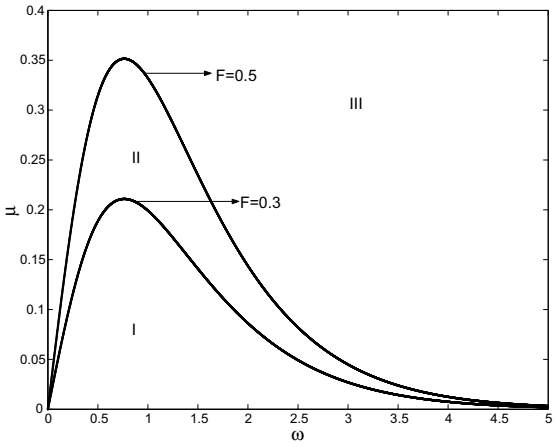

Fig. 3. Critical amplitude μ versus frequency for two different external amplitude parameter values.

quency parameter ω. The threshold of chaotic motion increases with the increasing of the external amplitude μ (Fig. 3). The region below the homoclinic bifurcation curve corresponding to $F = 0.3$ [region (I) of Fig. 3] represents the periodic orbits. When μ crosses its first critical value, a homoclinic bifurcation takes place, so that a hyperbolic Cantor set appears in a neighborhood of the saddles [regions (II) and (III) of Fig. 3]. The dynamics should therefore be chaotic only for large values of the damping. At the same time, when $F = 0.5$ [regions (I) and (II) of Fig. 3] it represents the periodic orbits, while the dynamics should therefore be chaotic in the region (III).

From Eq. (12), the chaotic behavior is guaranteed for the trajectories whose initial data are sufficiently near the unperturbed separatrix equation (9) if

$$\mu \leqslant \mu_{cr} = \frac{3\sqrt{2}F\pi\omega}{8}\operatorname{sech}\frac{\pi\omega}{2}, \tag{15}$$

where μ_{cr} is the threshold function.

4. Bifurcation analysis and fractal basins

4.1. Bifurcation diagram and Lyapunov exponent

Now we study the behavior of the system given by Eq. (2) as a function of the damping parameter for different values of the external perturbation. The bifurcation diagram and the maximal Lyapunov exponents have been represented for the variable x, and they can be seen in Fig. 4. A positive Lyapunov exponent for a bounded attractor is usually a sign of

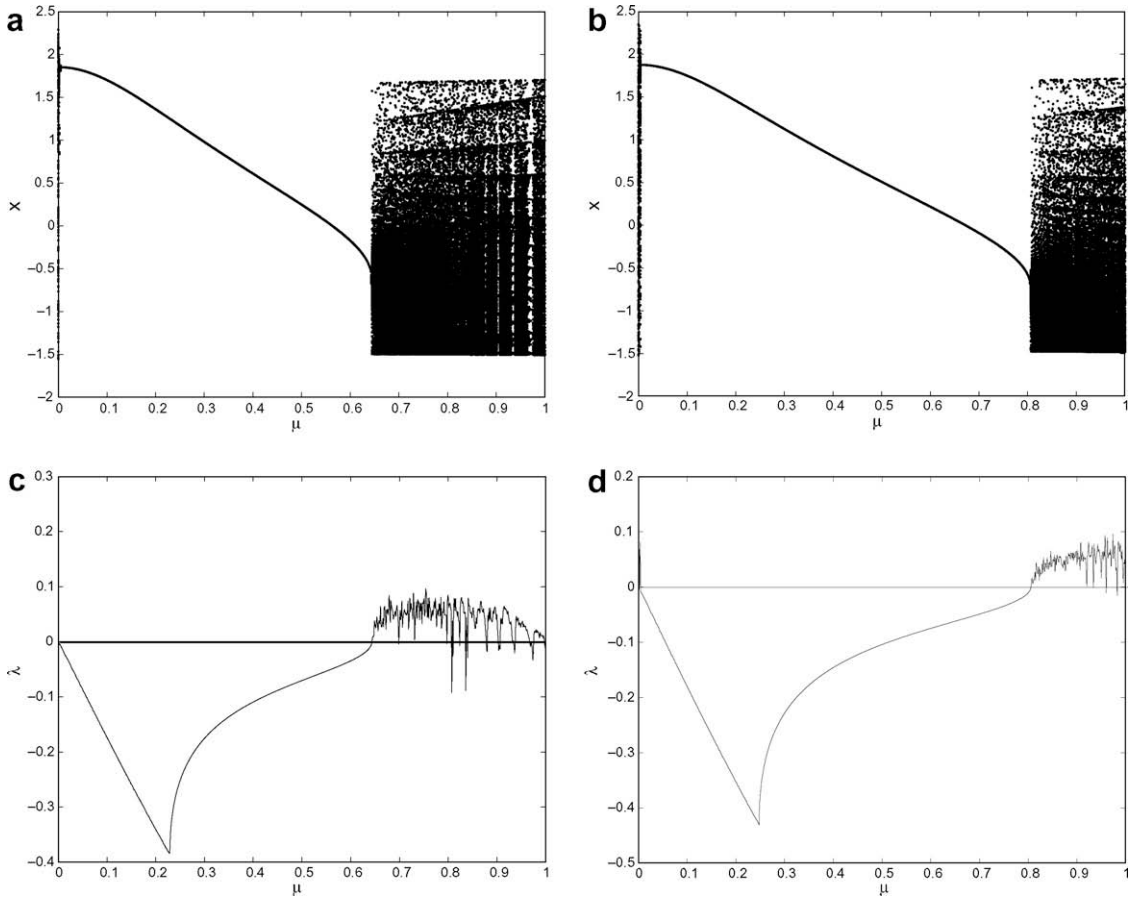

Fig. 4. (a,c) Bifurcation diagram and corresponding Maximal Lyapunov exponent of equation $\ddot{x} - \mu(1 - \dot{x}^2)\dot{x} - x + x^3 = 0.5\cos t$ as a function of μ; (b,d) bifurcation diagram and corresponding Maximal Lyapunov exponent of equation $\ddot{x} - \mu(1 - \dot{x}^2)\dot{x} - x + x^3 = 0.6\cos t$ as a function of μ.

chaos. We want to check the threshold of the external amplitude for the onset of possible chaos obtained in Section 3. For $\omega = 1$, the critical value of the external force has been obtained numerically for $F_{cr} = 0.5$. Above this value, numerical simulations have been carried out for the selected parameter values $F = 0.5$ (see Fig. 4a and c) and $F = 0.6$ (see Fig. 4b and d). From these figures, one can see that the thresholds of damping amplitude for the onset of chaos increase when the external amplitude increases above F_{cr}. As μ increases, the Lyapunov exponent changes from a negative value to a positive value, signifying the appearance of homoclinic chaos motion. The phase portrait of chaotic and periodic orbits have been plotted in Fig. 5.

4.2. Phase portraits and basins of attraction

In order to verify the analytical results obtained in the previous sections, we have numerically integrated the system by using a fourth order Runge–Kutta in order to investigate the homoclinic chaos in our model. We want to study what is the effect of using the nonlinear damping terms on the equation of the oscillator and how the basins of attraction are affected as the coefficient parameter μ is varied. To show the fractal structure, we consider the case of the bifurcation close to the resonance since it may undergo the limit cycles in the system. Hence we fix $F = 0.3$ and $\omega = 1$, the Melnikov threshold is given analytically by $\mu_{cr} \simeq 0.2$. Fig. 6 shows the basins of attraction of the forced Rayleigh–Duffing oscillator when $\mu = 0.6$ made by DYNAMICS [21]. Corresponding to the parameter value of $\mu = 0.6$ in the region (III) [Fig. 3], there exist two chaotic attractors represented by the grey and white colors, respectively. As we see from Fig. 6, the basin boundaries become fractal, which means that the damping parameter value μ has contributed to the fractalization of the boundaries, with the corresponding uncertainty associated to this fact.

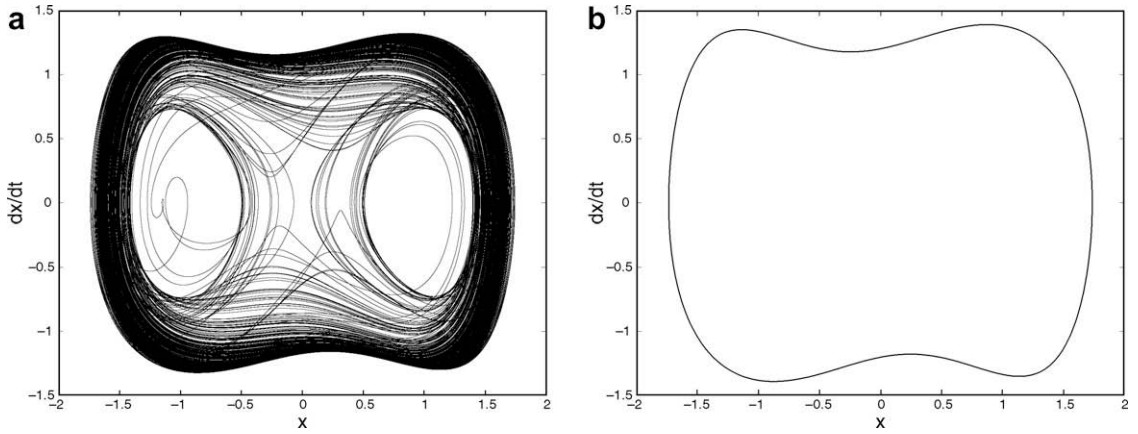

Fig. 5. Phase portraits corresponding to the system $\ddot{x} - \mu(1 - \dot{x}^2)\dot{x} - x + x^3 = 0.5\cos t$; (a) chaotic orbit $\mu = 0.695$, (b) Period-1 orbit $\mu = 0.5$.

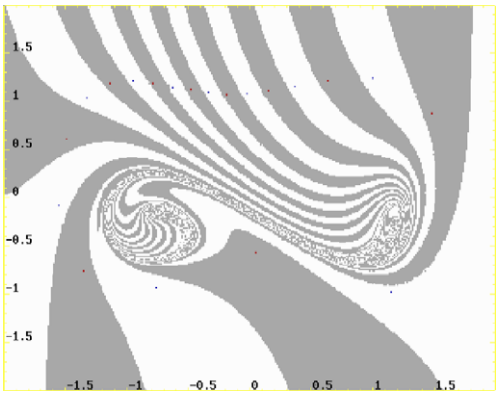

Fig. 6. Basin of attraction corresponding to the system $\ddot{x} - 0.6(1 - \dot{x}^2)\dot{x} - x + x^3 = 0.3\cos t$.

5. Summary and conclusions

We have carried out a detailed analysis of the criteria for the transition to chaotic motion of a combined Rayleigh and Duffing oscillator. The transition boundaries in the parameter space are obtained, which divide the space into different regions. In each region, the solutions are explored theoretically and numerically. The theory applicable to damping-induced chaotic dynamics reviewed in this paper rests primarily on the application of the Melnikov theory. The critical value of damping coefficient μ under which the system oscillates chaotically has been estimated, in the first step by means of the Melnikov method and later confirmed by calculating the corresponding Lyapunov exponent, bifurcation diagrams, and basin of attractions. Results were given for external periodic perturbation. By means of the basin of attraction, we have shown that for certain regions of parameter space, the deterministic system driven harmonically experiences behaviors that may be chaotic or non-chaotic.

The Melnikov method, is sensitive to a global homoclinic bifurcation and gives a necessary condition when the damping coefficient $\mu = \mu_{cr1}$ is larger than the critical homoclinic bifurcation values [19]. On the other hand, the largest Lyapunov exponent [22], measuring the local exponential divergence of particular phase portrait trajectories gives a sufficient condition $\mu = \mu_{cr2}$ for this transition which has obviously a higher value of the excitation amplitude $\mu = \mu_{cr2} > \mu_{cr1}$. Under the Melnikov transition prediction ($\mu < \mu_{cr1}$), we have obtained periodic windows as we expected drifting to transient chaos. This effect can be explained on the one hand by the fact that we have used the first order approximation perturbation, on the other hand by the nonlinearities of the damping. The present approach can be used to generalize models of magneto-rheological dampers in novel studies of their influence on vehicle dynamics [23]. To reduce harmful vibrations one can consider application of dampers composed of Duffing oscillator with the Rayleigh damping.

Acknowledgements

Martin Siewe Siewe acknowledges the warm hospitality at the Nonlinear Dynamics and Chaos Group of the Universidad Rey Juan Carlos where this work was carried out. The research was supported by the Spanish Ministry of Science and Technology under project Nr. BFM2003-03081 and by the Spanish Ministry of Education and Science under project Nr. FIS2006-08525.

References

[1] Guckenheimer J, Holmes PJ. Nonlinear oscillations, dynamical systems and bifurcation of vector fields. New York: Springer; 1983.
[2] Moon FC. Chaotic and fractal dynamics. New York: Wiley; 1992.
[3] Kao YH. Metamorphoses of basin boundaries in nonlinear dynamical systems. Phys Rev Lett 1986;59:1011.
[4] Feudel F, Witt A, Gellert M, Kurths J, Grebogi C, Sanjuán MAF. Intersections of stable and unstable manifolds: the skeleton of Lagrangian chaos. Chaos, Solitons & Fractals 2005;24:947.
[5] Sanjuán MAF. Subharmonic bifurcations in a pendulum parametrically excited by a non-harmonic perturbation. Chaos, Solitons & Fractals 1998;9:995.
[6] Sanjuán MAF. Remarks on transitions order-chaos induced by the shape of the periodic excitation in a parametric pendulum. Chaos, Solitons & Fractals 1996;7:435.
[7] Cao H, Seoane JM, Sanjuán MAF. Symmetry-breaking analysis for the general Helmholtz–Duffing oscillator. Chaos, Solitons & Fractals 2007;34:197–212.
[8] Trueba JL, Baltanás JP, Sanjuán MAF. A generalized perturbed pendulum. Chaos, Solitons & Fractals 2003;15:911.
[9] Vallejo JC, Mariño IP, Sanjuán MAF, Kurths J. Controlling chaos in a fluid flow past a moveable cylinder. Chaos, Solitons & Fractals 2003;15:255.
[10] Siewe MS, Kakmeni FMM, Tchawoua C. Resonant oscillation and homoclinic bifurcation in a Φ^6-Van der Pol oscillator. Chaos, Solitons & Fractals 2004;21:841.
[11] Siewe MS, Kakmeni FMM, Bowong S, Tchawoua C. Non-linear response of a self-sustained electromechanical seismographs to fifth resonance excitations and chaos control. Chaos, Solitons & Fractals 2006;29:431.
[12] Lazzouni SA, Siewe MS, Kakmeni FMM, Bowong S. Slow flow solutions and chaos control in an electromagnetic seismometer system. Chaos, Solitons & Fractals 2006;29:988.
[13] Ueda Y. Randomly transitional phenomena in the system governed by Duffing's equation. J Stat Phys 1979;20:181.
[14] Sanjuán MAF. The effect of nonlinear damping on the universal escape oscillator. Int J Bifurcat Chaos 1999;9:735.
[15] Pippard AB. The physics of vibration. Cambridge: Cambridge University Press; 1989.
[16] Munehisa S, Inaba N, Yoshinaga T, Kawakami H. Bifurcation structure of fractional harmonic entrainments in the forced Rayleigh oscillator. Electron Commun Jpn Part 3: Fundam Electron Sci 2004;87:30–40.

[17] Yamapi R. Synchronization dynamics in a ring of four mutually inertia coupled self-sustained electrical systems. Physica A 2006;366:187.
[18] Wang YC, Scott AG, James TS, MacDonald NC, Hartwell P, Bertsch F. Chaos in MEMS, parameter estimation and its potential application. IEEE Trans Circuits Syst I 1998;45:1013.
[19] Wiggins S. Introduction to applied nonlinear dynamical systems and chaos. New York, Heidelberg, Berlin: Springer-Verlag; 1990.
[20] Moon FC, Li GX. Fractal basin boundaries and homoclinic orbits for periodic motion in a two-well potential. Phys Rev Lett 1985;55:1439.
[21] Nusse HE, Yorke JA. Dynamics: numerical explorations, New York, 1998.
[22] Wolf A, Swift JB, Swinney HL, Vastano JA. Determining Lyapunov exponents from a time-series. Physica D 1985;16:285.
[23] Li S, Yang S, Guo W. Investigation of chaotic motion in histeric non-linear suspension system with multi-frequency excitations. Mech Res Commun 2004;31:229.